Article

Journal of the Brazilian Chemical Society

https://dx.doi.org/10.21577/0103-5053.20230166

J. Braz. Chem. Soc. **2024**, *35*, 4, e-20230166, 1-7

Study of the Three-Dimensional Structure of Tryptophan Zipper Peptides through ^{1}H NMR Chemical Shifts Calculations

Ana Carolina F. de Albuquerque *,[a] *and Fernando M. dos Santos Jr.* *,[a]

[a]*Departamento de Química Orgânica, Instituto de Química, Universidade Federal Fluminense (UFF), Outeiro de São João Batista, 24020-141 Niterói-RJ, Brazil*

Three-dimensional structures of proteins are intimately linked to their functions, therefore understanding their conformation in solution is essential. While nuclear magnetic resonance spectroscopy and X-ray crystallography are widely employed for protein structural determination, their limitations make the process challenging and expensive. Theoretical calculations of chemical shifts present a potential complement to experimental techniques, facilitating the study of protein structures. This investigation aims to assess the applicability of chemical shift calculations in analyzing three-dimensional structures of peptides, focusing on the tryptophan zipper 1 peptide as a model. Furthermore, a mutated variant of this peptide was proposed to evaluate the stability of its structural elements under sequence modifications. Through calculations, a potential structural alteration in the β-turn region of the mutant peptide compared to tryptophan zipper 1 was identified. This research demonstrates the potential of using computational approaches to complement experimental methods in studying protein structures and their functional implications.

Keywords: peptides, DFT, nuclear magnetic resonance, three-dimensional structure

Introduction

Most biological functions of proteins are directly linked to their primary structures and, consequently, to the spatial conformations they adopt in solution.[1] Therefore, studying the three-dimensional structures of proteins is crucial for a comprehensive understanding of their functions.[2] Throughout the 20th century, progress in biochemistry and experimental techniques resulted in the development of several methods for investigating the structure of proteins, including nuclear magnetic resonance (NMR) spectroscopy, X-ray crystallography, circular dichroism and cryogenic electron microscopy.[3-6]

In recent decades, the determination of three-dimensional structures through NMR spectroscopy has emerged as an alternative to X-ray crystallography, particularly for peptides and proteins that cannot be crystallized.[7] Protein structures have traditionally been determined based on homonuclear two-dimensional ^{1}H NMR spectra, on distances restraints acquired by nuclear Overhauser effects (NOE) experiments, and on dihedral angle restraints obtained from scalar spin-spin couplings and chemical shifts. However, the presence of a large number of signals in the same spectral region, resulting from the excessive number of protons even in small proteins, makes spectra assignment and structural determination arduous tasks.[8] Additionally, the line broadening due to fast spin nuclear relaxation in large proteins can difficult the acquisition of multidimensional spectra.[9]

In this context, the information derived from NMR chemical shifts, particularly those of ^{13}C, ^{1}H and ^{15}N nuclei, has proven to be of great significance in determining protein structures, as chemical shifts reflect the surrounding chemical environment of the nuclei. There is an empirical correlation between these parameters and the protein's secondary structure. Understanding these correlations and the impact of various structural effects on chemical shifts can offer crucial insights for characterizing protein structures.[8,10] Moreover, heteronuclear two- and three-dimensional (2D and 3D) spectra can provide information regarding chemical shift dispersions, which can be important in overcoming challenges associated with signal overlap.[11]

Recent developments in hardware and calculation methods (such as *ab initio* and density functional theories, along with hybrid approaches such as quantum mechanics/molecular mechanics (QM/MM))[12,13] have enabled the

*e-mail: acfalbuquerque@id.uff.br; fernando_martins@id.uff.br
Editor handled this article: Paula Homem-de-Mello (Associate)

use of QM theory for calculating NMR chemical shifts in peptide and protein structures. These simulated parameters have become important complementary tools to support experimental techniques in investigating protein structures. Consequently, it is now possible to establish precise relationships between calculated and experimental data, aiding spectra assignment and, ultimately, helping in the determination of three-dimensional protein structures. This significantly expands the scope of proteins that can be structurally characterized using NMR spectroscopy.[7,8]

In this work, our aim is to explore the feasibility of using NMR chemical shift calculations in the study of three-dimensional structures of peptides. To accomplish this, we have selected the peptide tryptophan zipper 1 (Trpzip 1; PDB ID: 1LE0) (Figure 1) as a model system, as its structure has been well characterized by NMR spectroscopy.[14-16] Additionally, the primary structure of Trpzip1, which consists of solely 12 amino acid residues, SWTWEGNKWTWK, is stabilized by four tryptophan residues, allowing the peptide to adopt a tertiary fold without the presence of ligand metals, unusual amino acids, or disulfide bonds. Therefore, Trpzip 1 proves to be an intriguing choice for structural investigations.[14] Moreover, in order to assess the stability of the three-dimensional structural elements in tryptophan zippers under sequence variations, we have proposed a peptide with a mutation in the primary structure of Trpzip 1. This mutation, in the region of the β-turn sequence, involved replacing the G-6 residue with an N residue, resulting in the following primary structure for the mutant peptide: SWTWE**NN**KWTWK.

Primary structure:

SWTWEGNKWTWK

Figure 1. Three-dimensional structure of Trpzip 1 (PDB ID: 1LE0).

Methodology

To explore the conformational space of the peptides, molecular dynamics (MD) simulations were performed using GROMACS v.4.5 software,[17-20] employing the CHARMM27 force field, as implemented in GROMACS.[21] The structures were placed in cubic boxes, with a volume of 1×10^3 Å, and the effects of water solvation in the biological environment were simulated using the TIP3P (transferable intermolecular potential with 3 points) water model.[22] The equilibrium phase of the simulation was divided into two steps. In the first step, the trajectory was simulated using the canonical ensemble (NVT), while the isothermal-isobaric ensemble (NPT) was used in the second step. During the equilibrium phase, the peptide structures were kept constrained, with their harmonic strengths fixed at their initial values. The trajectories were generated with 50,000 steps of 2 fs each. The leap-frog algorithm[23] was employed to integrate the equations of motion. To account for long-distance electrostatic interactions, the particle mesh Ewald (PME) method[24] was utilized. Temperature control was maintained using the Berendsen thermostat,[25] keeping the system at a constant temperature of 300 K. In the second equilibrium step, which employed the NPT ensemble, the Parrinello-Rahman barostat was used.[26] For the production phase of the simulation, the same parameters as the second equilibrium step (NPT ensemble) were used. This phase consisted of a total of 500,000 steps of 2 fs each, resulting in a total trajectory of 1 ns.

From the thermodynamically equilibrated classical trajectory, frames were selected at equal intervals of 100 ps, resulting in a total of 10 configurations. All frames were submitted to QM geometry optimizations, followed by ^{1}H nuclear magnetic shielding constants (σ) calculations.

Aiming to reduce the computational cost of the calculations, the system was partitioned using the QM/MM method,[13] using the Tcl ChemShell software[27] with Gaussian 16 interface,[28] for both geometry optimizations and ^{1}H NMR σ calculations. The peptide structures were fragmented into their respective amino acid residues. To preserve the chemical environment of the peptide bonds, the covalent bonds between the Cα atom and either the C' or N atoms of neighboring residues were fragmented without breaking the peptide bonds. As a result, each QM region contained individual residues. To account for the solvation effects, as experimental NMR data were obtained in a solution of 92% H_2O/8% D_2O,[14] all water molecules within a 5 Å range of the residue atoms were included in the QM region.

To determine the QM levels with the best compromise between accuracy and computational cost for peptide structure calculations, benchmark tests were conducted. Various QM Hamiltonians and basis sets available in the Gaussian interface within the Tcl ChemShell software[27] were evaluated for both geometry optimization and single-point NMR calculations. As a result, the ^{1}H NMR σ calculated with B3LYP/D95(d,p) level of theory, using

optimized geometries at HF/3-21G, provided the most favorable cost-effectiveness ratio. Hence, this level of theory was employed in the QM region of the QM/MM calculations. For the MM region, CHARMM27[21] force field was employed.

The calculated ^{1}H NMR σ values were used to obtain the chemical shifts (δ_{calc}) values, as $\delta_{calc} = \sigma_{DSS} - \sigma$, where σ_{DSS} is the shielding constant of the reference compound (sodium trimethylsilylpropanesulfonate, DSS) calculated using the same levels of theory as the Trpzip structures.

The same calculation procedures were applied to both Trpzip 1 and mutant peptides. For the Trpzip 1 calculations, a structure obtained from the Protein Data Bank (PDB)[15] (PDB ID: 1LE0) was used as the input geometry. It is worth noting that the PDB provided an ensemble of 20 conformers for Trpzip 1, as the structure was derived from NMR data. In this study, the geometry corresponding to conformer 1 was selected as the initial template for calculations, as it was established by the authors of the deposition, Cochran *et al.*,[14] as the most representative conformer in the ensemble. Regarding the mutant peptide calculations, the original geometry of Trpzip 1, specifically the first conformer from the ensemble deposited in the PDB, was used as the template model. Subsequently, in the PyMol software,[29] the G-6 residue was removed and replaced with an N.

Results and Discussion

Trpzip 1 is composed of a primary structure comprising 12 amino acid residues: SWTWEGNKWTWK (Figure 1). According to Cochran *et al.*,[14] its three-dimensional structure is characterized by a β-sheet fold, which consists of two antiparallel strands, connected by a β-turn. This particular conformation is referred to as β-hairpin.[5]

The Trpzip 1 structure, obtained from the PDB[15] (PDB ID: 1LE0), was used to conduct MD simulations. Once the frames were selected from the MD trajectory, they were used for the calculations of ^{1}H NMR chemical shifts. Table 1 shows both experimental (δ_{exp})[14] and calculated (δ_{calc}) ^{1}H chemical shifts, which were averaged across individual frames. Additionally, Table 1 includes the mean absolute deviation (MAD) and root mean square deviation (RMSD) values (0.81 and 1.08 ppm, respectively). The MAD and RMSD parameters were also calculated after excluding amide hydrogens, as these nuclei tend to be highly sensitive to experimental parameters such as temperature and intra/intermolecular hydrogen bonds. The resulting MAD value was 0.55 ppm, while the RMSD value was 0.67 ppm. The calculated ^{1}H chemical shift values for each individual frame can be found in the Supplementary

Table 1. Calculated [GIAO-B3LYP/D95(d,p)//HF/3-21G] (δ_{calc}) and experimental (δ_{exp}) ^{1}H chemical shifts obtained for Trpzip 1

Residue	Nuclei	δ_{calc} / ppm	δ_{exp} / ppm	$\lvert\delta_{exp} - \delta_{calc}\rvert$ / ppm
(1) Ser	Hα	3.80	3.40	0.40
	Hβ	4.22	3.69	0.53
(2) Trp	H^N	7.68	8.81	1.13
	Hα	4.69	5.20	0.51
	$Hβ^1$	3.44	3.02	0.42
	$Hβ^2$	2.96	3.13	0.17
(3) Thr	H^N	7.32	9.56	2.24
	Hα	4.98	4.85	0.13
	Hβ	4.44	3.99	0.45
(4) Trp	H^N	10.73	8.92	1.81
	Hα	4.90	4.61	0.29
	$Hβ^1$	3.50	2.07	1.43
	$Hβ^2$	3.08	2.94	0.14
(5) Glu	H^N	6.63	8.36	1.73
	Hα	4.43	4.34	0.09
	$Hβ^1$	1.44	1.75	0.31
	$Hβ^2$	2.20	1.87	0.33
(6) Gly	H^N	5.11	8.21	3.10
	$Hα^1$	4.28	3.48	0.80
	$Hα^2$	5.17	3.77	1.40
(7) Asn	H^N	10.32	8.14	2.18
	Hα	5.37	3.93	1.44
	$Hβ^1$	2.56	2.74	0.18
	$Hβ^2$	3.48	2.79	0.69
(8) Lys	H^N	7.48	6.53	0.95
	Hα	4.88	4.16	0.72
	$Hβ^1$	1.89	1.66	0.23
	$Hβ^2$	2.46	1.72	0.74
(9) Trp	H^N	8.50	8.55	0.05
	Hα	4.48	5.17	0.69
	$Hβ^1$	3.44	2.95	0.49
	$Hβ^2$	2.70	3.27	0.57
(10) Thr	H^N	7.35	9.77	2.42
	Hα	5.12	4.86	0.26
	Hβ	3.76	4.00	0.24
(11) Trp	H^N	10.32	9.00	1.32
	Hα	4.04	4.26	0.22
	$Hβ^1$	3.19	2.01	1.18
	$Hβ^2$	3.92	2.76	1.16
(12) Lys	H^N	7.12	7.73	0.61
	Hα	4.71	4.16	0.55
	$Hβ^1$	1.91	1.37	0.54
	$Hβ^2$	1.69	1.50	0.19
MAD[a]			0.81	
RMSD[a]			1.08	
MAD[b]			0.55	
RMSD[b]			0.67	

[a]Mean absolute deviation (MAD) and root mean square deviation (RMSD) values considering amide hydrogens; [b]MAD and RMSD values excluding amide hydrogens.

Information (SI) section (Table S1). Furthermore, the SI section provides a correlation graph of calculated *versus* experimental ^{1}H chemical shifts, including the R^2 (coefficient of determination) value and linear fitting (Figure S1). Finally, a 2D structural model of the amino acid sequence, indicating the analyzed hydrogen atoms for each residue, is presented in the SI section (Figure S3).

The comparison between the calculated and experimental chemical shifts resulted in MAD values below 1 ppm (0.81 ppm, including amide hydrogens, and 0.55 ppm, excluding these nuclei), indicating a good agreement. Additionally, the RMSD values were close to or below 1 ppm (1.08 ppm, including amide hydrogens, and 0.67 ppm, excluding these nuclei). These findings provide further confirmation that the chosen level of theory is suitable for structural investigations of tryptophan zipper peptides.

Considering that the calculated chemical shifts for the Trpzip 1 peptide accurately reproduced the experimental data, this methodology can be employed to assess the stability of the three-dimensional structure of tryptophan zippers when subjected to sequence variations. For this purpose, we proposed a theoretical modification to the primary structure of Trpzip 1, specifically within the region associated with the β-turn sequence. Our objective was to investigate whether the substitution of an amino acid residue would affect the type of β-turn present in the structure.

In a previous publication by Cochran *et al.*,[14] the synthesis of various tryptophan zipper peptides was reported. Among these peptides, three structures were distinguished solely by the substitution of two amino acid residues in the β-turn region. Consequently, these substitutions directly impacted the nature of this particular secondary structure element. In Trpzip1, the β-turn consisted of the amino acids EGNK, which the authors classified as type II'. Trpzip2 exhibited an alteration where the positions of the N and G residues were exchanged, resulting in the sequence ENGK and a type I' β-turn. Similarly, Trpzip3 presented a replacement of the G residue with p, giving rise to the sequence EpNK and maintaining a type II' β-turn, akin to the Trpzip1 structure.[14] In this study, our aim was to examine the effect of introducing an additional N amino acid by substituting one of the G residues. Consequently, the sequence of the mutant peptide is as follows: SWTWENNKWTWK.

Table 2 displays the calculated (δ_{calc}) ^{1}H chemical shift values, which represent the average of the values from each individual frame. Calculated ^{1}H chemical shift values for each individual frame are available in SI section (Table S2). Additionally, a 2D structural model of the amino acid sequence, indicating the hydrogen atoms analyzed for each residue, can be found in SI section (Figure S4).

Table 2. Calculated [GIAO-B3LYP/D95(d,p)//HF/3-21G] ^{1}H chemical shifts (δ_{calc}) obtained for the mutant peptide

Residue	Nuclei	δ_{calc} / ppm
(1) Ser	Hα	4.01
	Hβ	4.29
(2) Trp	H^N	8.33
	Hα	5.56
	$Hβ^1$	4.00
	$Hβ^2$	2.68
(3) Thr	H^N	7.80
	Hα	4.62
	Hβ	4.72
(4) Trp	H^N	10.05
	Hα	4.24
	$Hβ^1$	3.19
	$Hβ^2$	3.31
(5) Glu	H^N	7.54
	Hα	5.15
	$Hβ^1$	2.14
	$Hβ^2$	1.93
(6) Asn	H^N	9.71
	Hα	3.87
	$Hβ^1$	2.98
	$Hβ^2$	3.83
(7) Asn	H^N	6.95
	Hα	5.47
	$Hβ^1$	3.19
	$Hβ^2$	3.21
(8) Lys	H^N	7.27
	Hα	4.96
	$Hβ^1$	1.73
	$Hβ^2$	2.73
(9) Trp	H^N	7.72
	Hα	4.26
	$Hβ^1$	3.28
	$Hβ^2$	2.73
(10) Thr	H^N	7.52
	Hα	5.02
	Hβ	3.92
(11) Trp	H^N	9.20
	Hα	3.82
	$Hβ^1$	3.12
	$Hβ^2$	3.66
(12) Lys	H^N	7.72
	Hα	3.42
	$Hβ^1$	2.17
	$Hβ^2$	1.79

The degree of structural similarity between the folds of the mutant peptide and Trpzip 1 can be assessed through the analysis of ^{1}H chemical shifts. Backbone chemical shifts are sensitive to protein conformation, and different elements of secondary structure can exhibit distinct patterns of shielding and/or deshielding.[30,31] Therefore, these parameters can provide insights into changes in secondary structure elements. In this regard, differences in the ^{1}Hα chemical shifts between the mutant peptide and Trpzip 1 were compared to the random coil values, determined by Wishart *et al.*[32] (Figure 2). Experimental data from Trpzip 1[14] and calculated chemical shift values for the mutant peptide were used for this analysis.

The data presented in Figure 2 demonstrate that the mutant and Trpzip 1 peptides exhibit a similar pattern of differences in chemical shifts in relation to random coil values, with the exception of residues 5, 7, 8 and 9. In Trpzip 1, the Hα nuclei of residues 5, 7 and 8 are more shielded when compared to random coil structures. Conversely, the values for the mutant peptide display the opposite pattern. In contrast, in residue 9, the Hα nuclei of Trpzip 1 are more deshielded compared to random coil structures, while the values for the mutant peptide again exhibit the opposite trend.

The first three residues, 5, 7 and 8, comprise the β-turn region. From this observation, it can be inferred that the two peptides likely have similar conformations in the β-strand regions but exhibit different types of β-turns.

β-Turns are the most common type of turns and typically consist of four amino acid residues that connect two antiparallel β-strands,[5] as observed in the Trpzip 1 structure. Recently, Shapovalov *et al.*[33] identified the existence of 18 types of β-turns, which differ in the geometry of the peptide bonds in the 2nd and 3rd residues of the turn and in the distances between the Cα atoms of the 1st and 4th residues.[33] According to Cochran *et al.*,[14] in the case of Trpzip 1, the β-turn is composed of EGNK residues, resulting in a pD-type turn.

After identifying the potential change in the type of β-turn, the BetaTurnTool18 software[33,34] was employed to determine the most likely β-turn type in the structure of the mutant peptide. For comparison reasons, the software was also used to indicate the β-turn type present in the Trpzip 1 structure. To perform this analysis, the structure of the mutant peptide obtained from the MD simulations and the Trpzip 1 structure obtained from the PDB[15] (PDB ID: 1LE0) were used (Table 3).

The BetaTurnTool18 software, developed by Shapovalov *et al.*,[33,34] provides predictions on the most probable types of β-turn in protein structures. It takes the protein's coordinate file as input and calculates various parameters to determine the most likely β-turn type. These

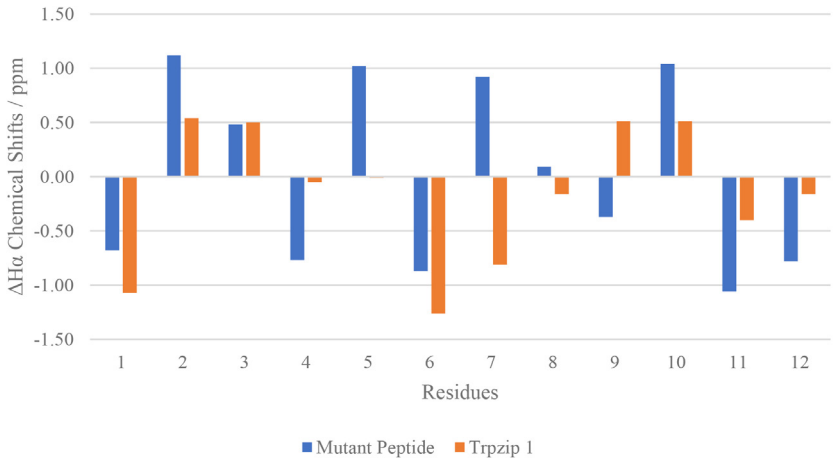

Figure 2. Differences between the chemical shifts of ^{1}Hα of the calculated structure for the mutant peptide (in blue) and the experimental structure of Trpzip 1 (in orange), in relation to the random coil values.

Table 3. Types of β-turns assigned to the calculated structure for the mutant peptide and for the experimental structure of Trpzip 1, confidence levels and values of angles Φ and Ψ

Peptide	Angle Φ / degree		Angle Ψ / degree		Type of β-turn	Confidence level
	Residue 2	Residue 3	Residue 2	Residue 3		
Mutant	167.59	179.97	69.79	–121.68	pD	9
Trpzip 1	89.12	–132.33	–56.90	–12.69	dD	5
					dN	4

parameters include the distance between the Cα atoms of the 1st and 4th residues of the β-turn, the hydrogen bond patterns within the β-turn residues, and the Φ and Ψ torsional angles of the 2nd and 3rd residues of the β-turn. The program assigns confidence levels to the identified β-turn types based on their distances to the first and second closest medoids. The confidence level is rated on a scale of 0 to 9, where 0 represents a confidence range of 0-10%, and 9 represents a confidence range of 90-100%. The authors[33] suggest that a confidence level of 7 or higher (70-80%) indicates a high probability of the assigned β-turn type. However, there are instances where certain β-turns may resemble multiple types. In such cases, the software indicates the two most likely types with confidence levels ranging from 0 to 6.[33,34]

As shown in Table 3, the BetaTurnTool18 software[34] assigned a pD-type β-turn to the mutant peptide with a high level of confidence (9). However, for Trpzip 1, which was initially classified as having a pD-type β-turn by Cochran *et al*.,[14] the software assigned two different types of turn, namely a dD and dN, both with high confidence levels. This suggests that the previous assignment of a pD-type β-turn for Trpzip 1 may potentially be inaccurate.[14]

This result clearly demonstrated the utility of quantum calculation of chemical shifts in assessing and identifying conformational changes in the three-dimensional structures of peptides and small proteins. It allows for obtaining significant structural information using a relatively fast and cost-effective theoretical method, without the necessity of prior syntheses and experiments, which would require time and resources.

A previous version of this article has been published as preprint.[35]

Conclusions

In this study, we investigated the applicability of ^{1}H chemical shift calculations for analyzing the three-dimensional structures of peptides, using Trpzip 1 as a model system. The calculations performed on the Trpzip 1 structure demonstrated that the selected level of theory (GIAO-B3LYP/D95(d,p)//HF/3-21G) accurately reproduced the experimental chemical shifts.

Given the accurate reproduction of experimental data through chemical shift calculations for Trpzip 1, we extended this methodology to evaluate the stability of the three-dimensional structure of tryptophan zippers against sequence changes. We applied the same level of theory to calculate chemical shifts for a mutant peptide with a sequence variation in Trpzip 1. The calculated data successfully identified a structural change in the β-turn region of the mutant peptide compared to Trpzip 1. Interestingly, our analysis suggests that the previously reported classification of β-turns in Trpzip1 might be incorrect, while the proposed mutant type exhibits the β-turn type previously assigned to Trpzip 1 (pD).

In conclusion, calculated ^{1}H chemical shifts proved to be a cost-effective tool with significant potential for studying the three-dimensional structures of peptides and small proteins.

Supplementary Information

Supplementary information is available free of charge at http://jbcs.sbq.org.br as PDF file.

Acknowledgments

The authors gratefully acknowledge the financial support of Conselho Nacional de Desenvolvimento Científico e Tecnológico and Coordenação de Aperfeiçoamento de Pessoal de Nível Superior (Financial Code 001).

References

1. Stollar, E. J.; Smith, D. P.; *Essays Biochem.* **2020**, *64*, 649. [Crossref]
2. Kuhlman, B.; Bradley, P.; *Nat. Rev. Mol. Cell Biol.* **2019**, *20*, 681. [Crossref]
3. Fernandez-Leiro, R.; Scheres, S. H. W.; *Nature* **2016**, *537*, 339. [Crossref]
4. Slabinski, L.; Jaroszewski, L.; Rodrigues, A. P. C.; Rychlewski, L.; Wilson, I. A.; Lesley, S. A.; Godzik, A.; *Protein Sci.* **2007**, *16*, 2472. [Crossref]
5. Kessel, A.; Ben-Tal, N. In *Introduction to Proteins: Structure, Function and Motion*, 2nd ed.; Kessel, A.; Ben-Tal, N., eds.; Taylor & Francis Group: New York, USA, 2018, ch. 2.
6. Milne, J. L. S.; Borgnia, M. J.; Bartesaghi, A.; Tran, E. E. H.; Earl, L. A.; Schauder, D. M.; Lengyel, J.; Pierson, J.; Patwardhan, A.; Subramaniam, S.; *FEBS J.* **2013**, *280*, 28. [Crossref]
7. Frank, A.; Onila, I.; Möller, H. M.; Exner, T. E.; *Proteins: Struct., Funct., Bioinf.* **2011**, *79*, 2189. [Crossref]
8. Mulder, F. A. A.; Filatov, M.; *Chem. Soc. Rev.* **2010**, *39*, 578. [Crossref]
9. Foster, M. P.; McElroy, C. A.; Amero, C. D.; *Biochemistry* **2007**, *46*, 331. [Crossref]
10. Wishart, D. S.; *Prog. Nucl. Magn. Reson. Spectrosc.* **2011**, *58*, 62. [Crossref]
11. Bermel, W.; Bruix, M.; Felli, I. C.; Kumar M. V. V.; Pierattelli, R.; Serrano, S.; *J. Biomol. NMR* **2013**, *55*, 231. [Crossref]
12. Field, M. J.; Bash, P. A.; Karplus, M.; *J. Comput. Chem.* **1990**, *11*, 700. [Crossref]

13. Warshel, A.; Levitt, M.; *J. Mol. Biol.* **1976**, *103*, 227. [Crossref]
14. Cochran, A. G.; Skelton, N. J.; Starovasnik, M. A.; *Proc. Natl. Acad. Sci. U. S. A.* **2001**, *98*, 5578. [Crossref]
15. The Research Collaboratory for Structural Bioinformatics Protein Data Bank, https://www.rcsb.org/, accessed in October 2023
16. Sehnal, D.; Bittrich, S.; Deshpande, M.; Svobodová, R.; Berka, K.; Bazgier, V.; Velankar, S.; Burley, S. K.; Koča, J.; Rose, A. S.; *Nucleic Acids Res.* **2021**, *49*, W431. [Crossref]
17. van der Spoel, D.; Lindahl, E.; Hess, B.; Groenhof, G.; Mark, A. E.; Berendsen, H. J. C.; *J. Comput. Chem.* **2005**, *26*, 1701. [Crossref]
18. Pronk, S.; Páll, S.; Schulz, R.; Larsson, P.; Bjelkmar, P.; Apostolov, R.; Shirts, M. R.; Smith, J. C.; Kasson, P. M.; van der Spoel, D.; Hess, B.; Lindahl, E.; *Bioinformatics* **2013**, *29*, 845. [Crossref]
19. Abraham, M. J.; Murtola, T.; Schulz, R.; Páll, S.; Smith, J. C.; Hess, B.; Lindahl, E.; *SoftwareX* **2015**, *1-2*, 19. [Crossref]
20. Bauer, P.; Hess, B.; Lindahl, E.; *GROMACS*, v.4.5; Royal Institute of Technology and Uppsala University, Sweden, 2022.
21. Mackerell Jr., A. D.; Feig, M.; Brooks III, C. L.; *J. Comput. Chem.* **2004**, *25*, 1400. [Crossref]
22. MacKerell, A. D.; Bashford, D.; Bellott, M.; Dunbrack, R. L.; Evanseck, J. D.; Field, M. J.; Fischer, S.; Gao, J.; Guo, H.; Ha, S.; Joseph-McCarthy, D.; Kuchnir, L.; Kuczera, K.; Lau, F. T. K.; Mattos, C.; Michnick, S.; Ngo, T.; Nguyen, D. T.; Prodhom, B.; Reiher, W. E.; Roux, B.; Schlenkrich, M.; Smith, J. C.; Stote, R.; Straub, J.; Watanabe, M.; Wiórkiewicz-Kuczera, J.; Yin, D.; Karplus, M.; *J. Phys. Chem. B* **1998**, *102*, 3586. [Crossref]
23. Amini, M.; Eastwood, J. W.; Hockney, R. W.; *Comput. Phys. Commun.* **1987**, *44*, 83. [Crossref]
24. Darden, T.; York, D.; Pedersen, L.; *J. Chem. Phys.* **1993**, *98*, 10089. [Crossref]
25. Berendsen, H. J. C.; Postma, J. P. M.; van Gunsteren, W. F.; DiNola, A.; Haak, J. R.; *J. Chem. Phys.* **1984**, *81*, 3684. [Crossref]
26. Parrinello, M.; Rahman, A.; *J. Appl. Phys.* **1981**, *52*, 7182. [Crossref]
27. Keal, T.; *ChemShell, a Computational Chemistry Shell*, v3.6; STFC Daresbury Laboratory, UK, 2014.
28. Frisch, M. J.; Trucks, G. W.; Schlegel, H. B.; Scuseria, G. E.; Robb, M. A.; Cheeseman, J. R.; Scalmani, G.; Barone, V.; Petersson, G. A.; Nakatsuji, H.; Li, X.; Caricato, M.; Marenich, A. V.; Bloino, J.; Janesko, B. G.; Gomperts, R.; Mennucci, B.; Hratchian, H. P.; Ortiz, J. V.; Izmaylov, A. F.; Sonnenberg, J. L.; Williams-Young, D.; Ding, F.; Lipparini, F.; Egidi, F.; Goings, J.; Peng, B.; Petrone, A.; Henderson, T.; Ranasinghe, D.; Zakrzewski, V. G.; Gao, J.; Rega, N.; Zheng, G.; Liang, W.; Hada, M.; Ehara, M.; Toyota, K.; Fukuda, R.; Hasegawa, J.; Ishida, M.; Nakajima, T.; Honda, Y.; Kitao, O.; Nakai, H.; Vreven, T.; Throssell, K.; Montgomery Jr., J. A.; Peralta, J. E.; Ogliaro, F.; Bearpark, M. J.; Heyd, J. J.; Brothers, E. N.; Kudin, K. N.; Staroverov, V. N.; Keith, T. A.; Kobayashi, R.; Normand, J.; Raghavachari, K.; Rendell, A. P.; Burant, J. C.; Iyengar, S. S.; Tomasi, J.; Cossi, M.; Millam, J. M.; Klene, M.; Adamo, C.; Cammi, R.; Ochterski, J. W.; Martin, R. L.; Morokuma, K.; Farkas, O.; Foresman, J. B.; Fox, D. J.; *Gaussian 16, Revision C.01*; Gaussian, Inc., USA, 2016.
29. *The PyMOL Molecular Graphics System*, version 2.0; Schrödinger, LLC, USA, 2018.
30. Huang, R.; Wu, L.; McElheny, D.; Bouř, P.; Roy, A.; Keiderling, T. A.; *J. Phys. Chem. B* **2009**, *113*, 5661. [Crossref]
31. de Dios, A. C.; *Prog. Nucl. Magn. Reson. Spectrosc.* **1996**, *29*, 229. [Crossref]
32. Wishart, D. S.; Bigam, C. G.; Holm, A.; Hodges, R. S.; Sykes, B. D.; *J. Biomol. NMR* **1995**, *5*, 67. [Crossref]
33. Shapovalov, M.; Vucetic, S.; Dunbrack Jr., R. L.; *PLoS Comput. Biol.* **2019**, *15*, e1006844. [Crossref]
34. Shapovalov, M.; Vucetic, S.; Dunbrack Jr., R. L.; *BetaTurnTool18*, v.1.1.10; Temple University, USA, 2019
35. de Albuquerque, A. C. F.; dos Santos Jr., F. M.; *Research Square*, 2022. [Link] accessed in October 2023

Submitted: June 20, 2023
Published online: October 17, 2023